Quantum Optical Control of Donor-bound Electron Spins in GaAs

Sladkov, Maksym

Chapter 7

Ultrafast preparation and detection of coherent dark states in low-doped n-GaAs

We report an optical pump-probe study of spin coherence of donor-bound electrons in GaAs. We find that single pump pulses prepare the spins in a coherent dark state via an ultra-fast stimulated Raman process. Two orthogonal polarization components in the pump pulses each address one leg of the Raman system. The phase and amplitude difference between these components govern which spin state is prepared, and we can prepare any superposition of spin states. This preparation occurs 1000 times faster than the system's spontaneous emission and decoherence times. The fast preparation and detection of these coherent states allows for a direct time-resolved study of the coherent dynamics and dephasing of the electron spin in this system, which is difficult to study with other optical methods.

7.1 Introduction

In order to implement quantum algorithms for computing, one has to follow the same approach as for developing a classical computer in several ways. The state upon which the quantum operation has to be performed first has to be initialized, then manipulated, and eventually read. All these three ingredients are crucial for creating an operational quantum computer, and were tackled together or separately in different physical systems with different levels of success [1]. Existing research on creating registers for quantum information includes systems where a bit of information is stored on a degree of freedom of a single particle, like the polarization state of an optical photon [2], the quantum state of a trapped atom [3], the electron spin state in a semiconductor quantum dot [4, 5], the nuclear spin state of an individual paramagnetic dopant in silicon [6], and the spin state of an NV center in diamond [7]. Other types of qubits include those that store quantum information on the state of an ensemble of particles with many degrees of freedom, as in NMR based quantum computers [8–10] and quantum computing with macroscopic states of superconducting currents in Josephson junction circuits [11].

Work on spin ensembles in n-GaAs includes successful experiments on ultrafast spin rotations by means of detuned optical pulses [12–14]. In those experiments the initial state of the spin ensemble was prepared in a pure state (ground state of the spin system) by means of optical pumping [5, 15] and then rotated using a dynamic ac-Stark shift that is caused by a detuned optical pulse [16, 17]. The spin rotation does happen on a time scale that is set by the optical Rabi frequency that is associated with the optical pulse, which can easily reach more than 100 GHz. What is limiting the overall performance in time is the preparation step, which requires a few cycles of the system's spontaneous emission time for the optical transitions. This is $T_{rad} = 1$ ns for donor-bound excitions in GaAs [18]. Much faster preparation is crucial in situations where qubits need to be re-prepared during a computation, as for example in quantum error-correction schemes.

In this Chapter we present an experiment where, by means of ultrafast optical pulses that are tuned in resonance with optical transitions, we can prepare an arbitrary coherent spin state in a donor-bound electron ensemble. The preparation occurs via a stimulated Raman process, on a time scale which is set by the optical Rabi frequency and which is about 1000 times faster than the system's radiative lifetime. In contrast to the use of detuned optical pulses for spin rotation via the ac-Stark effect, where only virtual optical transitions are excited that do not result in actual population of the optically excited state, in our scheme the resonant pulses drive strong Rabi transitions that cause actual population of the excited states. In this Chapter we study this ultra-fast preparation mechanism, and

investigate whether it can be useful in quantum information processing.

In order to study the preparation and subsequent coherent dynamics of the spin ensembles we employ the Time-Resolved Kerr Rotation (TRKR) technique [19–22]. This is widely used in studies of spin dynamics of electrons in the conduction band of semiconductors. In these studies, electron spin coherence is created with an optical pump pulse tuned at or just above the band gap, and this process injects spin-oriented photo-electrons in the conduction band. Detection in this scheme relies on the rotation of the linear polarization of a probe pulse upon reflection. This rotation is caused by the dependence of the absorbtion coefficient and the refractive index on the state of the electron spins, due to the polarization selection rules that apply for these electron-hole excitations [23]. For our experiment, we used pump pulses that are resonant with the D^0-D^0X transitions, which do not inject photo-electrons in the conduction band. We will investigate in this Chapter how the TRKR signal depends on the polarizations for pump and probe in the case of the D^0-D^0X transitions. This analysis has a close link to EIT-like physics that occurs during the presence of the optical pulses, and we find that we can prepare the ensemble in a coherent dark state that is purely determined by the polarization state of the pump pulse. We also make a first step towards explaining how the probe pulse is probing the spin coherence of these donor-bound electrons.

7.2 Spectral properties of D^0 electron spin system

The electron that is bound at a neutral donor site is described by a hydrogen-like envelope wavefunction, and the ground state has the s-type spherical symmetry. This D^0 electron has a first excited state with a p-type symmetry, and optical transitions of the D^0-D^0X type associated with this p-level of the D^0 electron are 2 nm (3.7 meV) red shifted with respect to the transitions from the D^0-1s orbital. When a magnetic field is applied, the ground state of the D^0 is Zeeman split into $|g\rangle = |\uparrow\rangle$, characterized by the angular momentum projection quantum number $m_e = +1/2$, and $|s\rangle = |\downarrow\rangle$ with $m_e = -1/2$ for this quantum number.

In order to address the electron spin states optically we use optical transitions from the D^0 state to the donor-bound exciton state D^0X. This D^0X state consists of two electrons forming a singlet and a heavy hole, and is denoted as $|\downarrow\uparrow, m_h\rangle$. The spins of a pair of electrons in a singlet state do not contribute to angular momentum. The heavy hole has a total angular momentum of $J_h = 3/2$, and the angular momentum projection quantum number can take a value in the range $m_h = -3/2...+3/2$. We again assume that a magnetic field is applied. In order to then describe the energy levels of the donor-bound exciton system (the D^0X levels

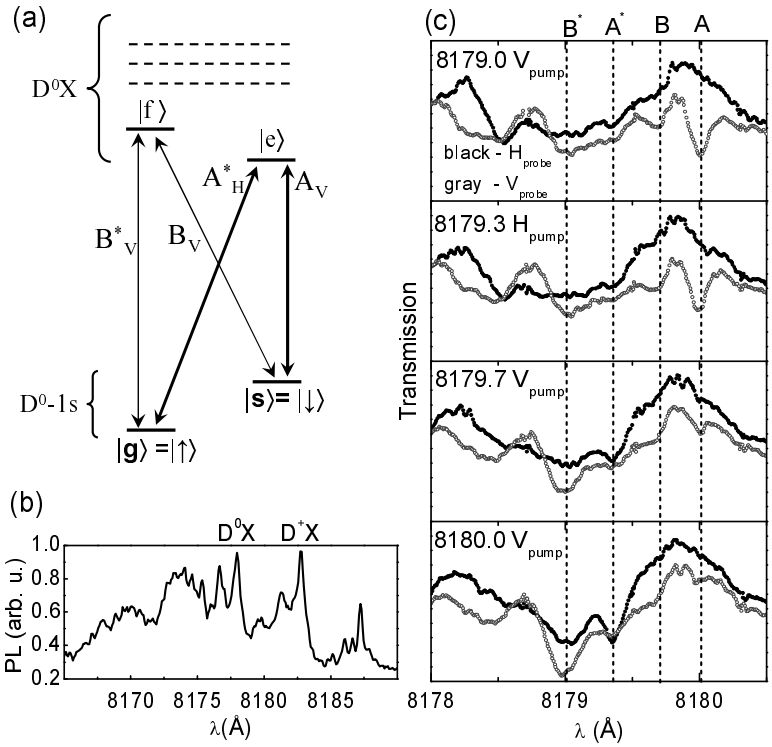

Figure 7.1: (a) The many-level system and optical transitions for the $D^0 - D^0X$ excitations in GaAs. The letter V indicates that a transition is sensitive to the vertical polarization, while the letter H indicates sensitivity to the horizontal polarization. (b) Photoluminescence collected from the n-GaAs sample in a magnetic field of $B = 7$ T. (c) Pump-assisted transmission spectroscopy of the $D^0 - D^0X$ system. The pump wavelength and polarization appear as labels in the top-left of panels. Gray (black) traces are results obtained with H (V) polarization for the probe.

in Fig. 7.1(a)), the orbital excited states of the envelope wavefunction also have to be taken in account [24]. This, in turn, leads to a very complicated level structure for the D^0X complex and there is at this stage no consensus in the community on labeling the states with angular momentum quantum numbers. From systematic magneto-luminescence studies it was concluded that the lowest level of the D^0X complex corresponds to $m_h = -3/2$, while the first excited state has $m_h = -1/2$ with the orbital quantum number $L = 1$ [24]. Other studies, however, are not uni-

vocal with these findings and are using alongside similar labeling [18] the labeling where the lowest level of the D^0X complex has $m_h = -1/2$, as in our findings (Chapter 6 and Ref. [25]), while the first excited state is reported to be $m_h = -3/2$ [26].

In general, the knowledge of the quantum numbers allows to determine polarization selection rules in optical spectra (Chapter 3). Considering, however, the ambiguity of the angular momentum quantum numbers we performed a pump-assisted optical spectroscopy experiment to determine the optical selection rules. For this experiment we used two CW wavelength-tunable lasers that have perpendicular incidence on the sample surface. The magnetic field is applied in the plane of the sample and the polarization of both lasers is chosen to be linear. When the laser light is V polarized, namely its polarization is parallel to the applied magnetic field, it induces π-type optical transitions without a change in the angular momentum quantum number, $\Delta m = 0$. When the laser light is H polarized (orthogonal to the magnetic field) it induces σ-type optical transitions with a change in angular momentum quantum number $\Delta m = \pm 1$ (Chapter 3). This is the same experiment as was described in the Chapter 6 previously.

First, we find the spectral position of the $D^0 - D^0X$ transitions by performing a photoluminescence experiment. We excited the sample above the band gap with $\lambda_{exc} = 805$ nm light and detect photoluminescence using an Acton 750 spectrometer equipped with a nitrogen cooled CCD camera. The distinct bands of the free (X), neutral donor-bound (D^0X), and charged donor-bound (D^+X) excitons are observed, as shown in Fig. 7.1(b).

For the pump-assisted transmission spectroscopy one of the CW lasers (either H or V polarized) is set to optically pump into one of the D^0X transitions, while the other CW laser scans across the region of the donor-bound exciton absorption. We collect transmission spectra in both H and V polarization, while pumping in the first four D^0X transitions (Fig. 7.1(c)). From this pump-assisted spectroscopy study we can conclude that the first four transitions arise from the level scheme depicted in Fig. 7.1(a). When pumping with V-polarized light into the transition A, which is at 8180.00 Å, we see an enhancement in absorbtion for the transition A^* at 8179.30 Å for H-polarized probe light. This pair of transitions constitutes a so-called Λ-system, which we label as $A - A^*$. In the same manner we can identify a Λ-system with the pair of transitions labeled as $B - B^*$. The fact that all four of these transitions are can be spectrally resolved, and are sensitive to either V- or H-polarization, allows for implementing control of the D^0 electron spin: The $A - A^*$ system couples the electron spin states $|\uparrow\rangle$ and $|\downarrow\rangle$ to the common excited state $|e\rangle$, while the $B - B^*$ system couples the same electron spin states to the common excited state $|f\rangle$.

Since we experimentally identified the polarization selection rules we can pro-

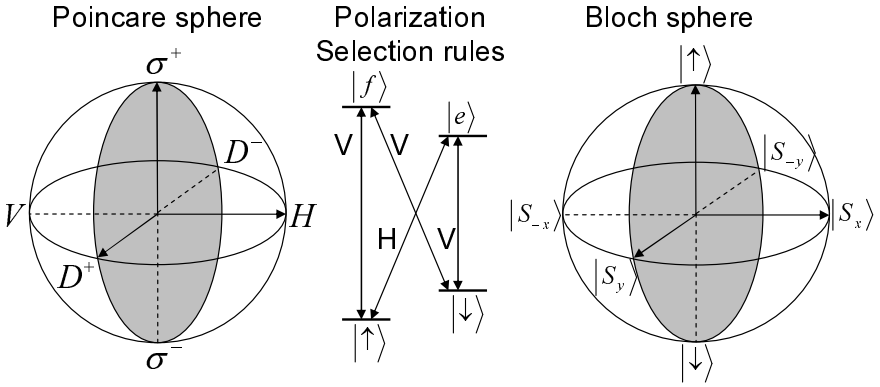

Figure 7.2: Poincare sphere for describing the light polarization state vector, and the Bloch sphere for describing the electron-spin state vector. The level scheme summarizes the polarization selection rules that determine the mapping between polarization states and spin states.

ceed with our study without having certainty about the proper labeling of angular momentum quantum numbers to the D^0X levels. For the sake of book-keeping, and based on our results, we can determine that the state $|e\rangle$ corresponds has $m_h = -1/2$. The the state $|f\rangle$ couples to both electron spin states via V-polarized transitions, and this sets a fundamental difficulty for determining its angular momentum quantum number since V-polarized light is expected to drive optical transitions with $\Delta m = 0$ (see also Chapter 3).

7.3 The coherent dark state for an electron spin in the optically driven Λ-system

In order to describe how optical orientation of the D^0 electron spin occurs while driving the $D^0 - D^0X$ transitions we have to consider the pair of transitions $A - A^*$ (or $B - B^*$) that constitute a Λ-system. We first consider two optical fields with polarizations that are chosen such that each fields is coupling to one of the optical transitions in the Λ-system. The optical Rabi frequencies of the two fields are denoted as Ω_1 and Ω_2 when both fields are on resonance with their transitions. Further, the $D^0 - D^0X$ system is characterized by a fast radiative lifetime and relatively long dephasing time for the spin in the ground state. Such a system has a

coherent dark state, which is:

$$|\Psi_{Dark}\rangle = \frac{1}{\sqrt{|\Omega_1|^2 + |\Omega_2|^2}} (\Omega_1|\downarrow\rangle + \Omega_2|\uparrow\rangle) \tag{7.1}$$

When the system is in this state, destructive quantum interference between the two optical transitions prohibits population of the optically excited state, as was demonstrated in the EIT experiment in Chapter 6 [25]. The system's tendency to evolve into this dark state was also observed as coherent population trapping, in spectroscopic measurements of photoluminescence from $D^0 - D^0X$ systems [18]. However, these experiment studied the steady-state response from driving with CW lasers, and do not give direct insight into the dynamics that brings the systems into this dark state, but this can be derived from the modeling that was presented in Chapter 4: If the spins are initially in a completely arbitrary but fully incoherent state, the $D^0 - D^0X$ systems will, in general, initially show some optical excitation after switching on the fields that drive the two transitions. Due to the damping of this dynamics from spontaneous emission, the system gradually evolves into the dark state, over a time scale that is a few times the spontaneous emission time (several nanoseconds). This seems to indicate that preparing an initially mixed spin state in the the dark state can not be carried with a picosecond pulse. We further comment on this after first discussing how the phase and amplitude of the two laser fields determine the actual spin orientation that corresponds to the dark state.

As can be seen from the Equation 7.1 the dark state depends solely on the phase and the amplitude of the optical Rabi frequencies of the two optical driving fields. It is easy to note that the dark state for $\Omega_1 = \Omega_2$ corresponds to maximum electron spin coherence, since it can be depicted on the electron spin Bloch sphere as a vector in the equatorial plane (Fig. 7.2). If both Ω_1 and Ω_2 are real numbers, which is equivalent to the having no phase difference between the two optical fields, the orientation of the dark state is collinear with the direction of the optical field propagation (x-direction), and results in a preparation of the spin state along the x-direction. This state is the superposition $|S_x\rangle = \frac{1}{\sqrt{2}}(|\uparrow\rangle + |\downarrow\rangle)$. In order to satisfy the condition that $\Omega_1 = \Omega_2$ on the $A - A^*$ system one optical field must have V polarization, while the other must have H polarization. Control over the amplitudes of the Rabi frequencies is done via changing the intensity of the fields. In a similar fashion one can generate a dark state that will correspond to the S_y spin state, which is the superposition $|S_y\rangle = \frac{1}{\sqrt{2}}(|\uparrow\rangle + i|\downarrow\rangle)$ superposition and therefore requires a $\pi/2$ phase shift between Ω_1 and Ω_2.

This phase shift can be controlled very well when the optical fields are derived from a single laser pulse, that is spectrally broad due to its short duration. This can

be applied when the spectral width of the pulse is larger than the Zeeman splitting of the electron spin, and when the central frequency of the pulse is such that the absolute value of the associated detunings for both transitions of the Λ-system are equal. A phase difference of 0 between Ω_1 and Ω_2 is then achieved when the laser light is linearly polarized along the direction $\frac{1}{\sqrt{2}}(H+V)$. A phase difference of $\pi/2$ between Ω_1 and Ω_2 is achieved when the laser light is $\sigma+$ polarized, since this can be presented as a superposition of the two linear polarizations as $\sigma+ = \frac{1}{\sqrt{2}}(H+iV)$.

These relations between polarization and spin orientation of the dark state can be pictured using a vector that represents the polarization on the Poincare sphere, and a similar vector for the spin state on the Bloch sphere (Fig. 7.2). This shows that by choosing the appropriate phase difference and relative amplitudes for the H and V components in a short laser pulse, the coherent dark state can correspond to any spin state of the D^0 system. The next Section discusses how this coherent dark state plays a role in the system's dynamics in response to a picosecond laser pulse.

7.4 Theory of the fast dark state preparation using picosecond optical pulses

When the $D^0 - D^0X$ system is subject to excitation by a picosecond optical pulse, the presence of the optical field during the pulse favors evolution into the dark state. We will concentrate here on the scenario where we assume a completely mixed spin state for the initial D^0 spin state, because this matches best with the experimental finding that are reported in the following Section. In this case, there is little rotational dynamics for the spin during the picosecond pulse, which would typically result in the situation that the spin orientation at the end of the pulse shows a strong dependence on the pulse area, and that is not observed (the spin part of such dynamics that occurs in parallel with coherent optical transitions is in fact precession of the spin about the axis that is defined by the dark state, such that any damping also results in evolution towards the dark state). With this assumption, a picosecond pulse can indeed show robust driving into the dark state. However, owing to the short duration of the pulse $T_{pulse} = 0.1 - 10$ ps as compared to the radiative relaxation times in the system $T_{rad} = 1$ ns, the population of the coherent dark state will still be a function of the strength of the optical field and duration of the pulse, which, as will be shown, reflects the coherent dynamics of the $D^0 - D^0X$ in a strong optical field.

In order to describe the dynamics of the $D^0 - D^0X$ system we have chosen to

solve the equation of motion for a density matrix defined on a 4-level system as in Fig .7.3: $|g\rangle$, $|s\rangle$ - electron spin states and $|e\rangle$, $|f\rangle$ - the ground and the first excited state of the D^0X complex, respectively. The 4-level system under consideration consist of the two Λ-systems labeled previously as $A-A^*$ and $B-B^*$ in Fig. 7.3. We have chosen to extend the number of levels in the present model, as compared to the 3-level model we have used for the EIT experiment (Chapter 6), because in the EIT experiment the use of CW lasers assures decoupling of the optical fields from the transitions that are outside the 3-level Λ-system. When picosecond optical pulses are used the linewidth of the laser is about $\Delta\lambda = 1$ nm, which results in coupling to several excited states of the D^0X complex. However, we restrict our analysis to a model that incorporates only 4 levels (2 for D^0 and 2 for D^0X), since this gives access to investigating the essential deviations from the dynamics of the 3-level system in a tractable manner, without too many parameters. The experimental results show in fact behavior that to a large extend matches with 3-level dynamics, with only a few small deviations. This indicates that the lowest levels of the D^0X complex are most important for the system's dynamics during a resonant optical pulse. In addition, we have indications that inter-level relaxation within the D^0X complex is very fast (further discussed below), including fast relaxation from the state $|f\rangle$ to the state $|e\rangle$, and this allows for considering the state $|f\rangle$ as one that describes effectively all the above lying states of the D^0X complex.

The equation of motion for the density matrix is:

$$\frac{d\hat{\rho}}{dt} = -\frac{i}{\hbar}\left[\hat{H}_{total}, \hat{\rho}\right] + \hat{L}\left(\hat{\rho}\right) \tag{7.2}$$

where and $\hat{H}_{total}$ is the Hamiltonian and $\hat{L}\left(\hat{\rho}\right)$ the Lindblad relaxation operator. The Hamiltonian describes the bare matter system and the driving by coherent laser fields, and will be described in the rotating frame under the rotating wave approximation (which is strictly speaking not valid in the situation that is considered, but still a good approximation because each transition most strongly responds to a fully resonant contribution in the pulse spectrum). The Hamiltonian then reads:

$$\hat{H} = \hbar \begin{pmatrix} 0 & 0 & -\Omega_1^* & -\Omega_3^* \\ 0 & \delta & -\Omega_2^* & -\Omega_4^* \\ -\Omega_1 & -\Omega_2 & \Delta_1 & 0 \\ -\Omega_3 & -\Omega_4 & 0 & \delta_{EF} \end{pmatrix} \tag{7.3}$$

where Δ_1 is the detuning of the optical field from the $g-e$ transition, δ is the two-photon detuning from the electron-Zeeman splitting and δ_{EF} is the two-photon detuning from the ground and excited state splitting of the D^0X states. Ω_1, Ω_2, Ω_3 and Ω_4 are the optical Rabi frequencies induced by the field of the optical pulse

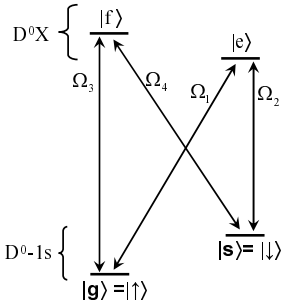

Figure 7.3: The 4-level system that is used for theoretical model

on the transitions $g-e$, $s-e$, $g-f$ and $s-f$ respectively. The optical pulse has temporal width ΔT and is assumed to be Fourier limited with a Gaussian profile characterized by the spectral width ΔE such that $\Delta E >> E_{gs} \gtrapprox E_{ef}$, where E_{gs} is the electron-spin Zeeman splitting, and E_{ef} the energy splitting between the two D^0X levels.

The relaxation operator is:

$$\hat{L}(\hat{\rho}) = \left(\begin{array}{l} -\Gamma_{gs}\rho_{gg} + \Gamma_{sg}\rho_{ss} + \Gamma_{eg}\rho_{ee} + \Gamma_{fg}\rho_{ff} \\ -\left(\left(\Gamma_{gs}+\Gamma_{sg}\right)/2+\gamma_s\right)\rho_{sg} \\ -\left(\left(\Gamma_{gs}+\Gamma_{eg}+\Gamma_{es}+\Gamma_{fe}\right)/2+\gamma_e\right)\rho_{eg} \\ -\left(\left(\Gamma_{gs}+\Gamma_{eg}+\Gamma_{es}+\Gamma_{fe}\right)/2+\gamma_f\right)\rho_{fg} \\ \quad -\left(\left(\Gamma_{gs}+\Gamma_{sg}\right)/2+\gamma_s\right)\rho_{gs} \\ \quad \Gamma_{gs}\rho_{gg} - \Gamma_{sg}\rho_{ss} + \Gamma_{es}\rho_{ee} + \Gamma_{fs}\rho_{ff} \\ \quad -\left(\left(\Gamma_{sg}+\Gamma_{eg}+\Gamma_{es}+\Gamma_{fe}\right)/2+\gamma_e\right)\rho_{es} \\ \quad -\left(\left(\Gamma_{gs}+\Gamma_{es}+\Gamma_{fs}+\Gamma_{fe}+\Gamma_{fg}\right)/2+\gamma_f\right)\rho_{fs} \\ \quad\quad -\left(\left(\Gamma_{gs}+\Gamma_{eg}+\Gamma_{es}\right)/2+\gamma_e\right)\rho_{ge} \\ \quad\quad -\left(\left(\Gamma_{sg}+\Gamma_{eg}+\Gamma_{es}\right)/2+\gamma_e\right)\rho_{se} \\ \quad\quad -\left(\Gamma_{eg}+\Gamma_{es}+\Gamma_{ef}\right)\rho_{ee} + \Gamma_{fe}\rho_{ff} \\ \quad\quad -\left(\left(\Gamma_{fe}+\Gamma_{ef}+\Gamma_{fs}+\Gamma_{fg}\right)/2+\gamma_X\right)\rho_{fe} \\ \quad\quad\quad -\left(\left(\Gamma_{gs}+\Gamma_{eg}+\Gamma_{es}+\Gamma_{fe}\right)/2+\gamma_f\right)\rho_{gf} \\ \quad\quad\quad -\left(\left(\Gamma_{gs}+\Gamma_{es}+\Gamma_{fs}+\Gamma_{fe}+\Gamma_{fg}\right)/2+\gamma_f\right)\rho_{sf} \\ \quad\quad\quad -\left(\left(\Gamma_{fe}+\Gamma_{ef}+\Gamma_{fs}+\Gamma_{fg}\right)/2+\gamma_X+\right)\rho_{ef} \\ \quad\quad\quad -\left(\Gamma_{fg}+\Gamma_{fs}+\Gamma_{fe}\right)\rho_{ff} + \Gamma_{ef}\rho_{ee} \end{array} \right) \quad (7.4)$$

where $\Gamma_{sg} = \left(2.6\,\mu\text{s}\right)^{-1}$ is the longitudinal spin relaxation rate, $\Gamma_{gs} = \Gamma_{sg} e^{E_{gs}/kT}$, $\Gamma_{eg} = \Gamma_{fg} = \Gamma_{es} = \Gamma_{fs} = (1\text{ ns})^{-1}$ are the radiative relaxation rates from the D^0X levels to the D^0 spin levels, $\gamma_{gs} = (0.3\text{ ns})^{-1}$ is the electron spin dephasing rate, which is shorter than for the EIT experiment from the Chapter 6 as a consequence of using a spectrally broad optical pulse, as will be shown at the end of this Chapter, $\gamma_{eg} = \gamma_{es} = \gamma_{fg} = \gamma_{fs} = 6$ GHz represent inhomogeneous optical broadening and $\gamma_{fe} = (1\text{ ps})^{-1}$ is the hole spin dephasing time.

An important parameter in our model is $\Gamma_{fe} = (1\text{ ps})^{-1}$, the rate for relaxation within the D^0X complex. We have to choose it to be very large, because, as will be shown in the experiment, with respect to the pump the system behaves like a 3-level system ($A - A^*$ part only). In order to describe response of the probe, however, all 4 levels need to be taken into account. We note that the assumption of the very fast relaxation is inconsistent with optical spectroscopy that was performed on this system since it would result in a transition linewidth as large as 1 THz, while in reality it was never observed to exceed the value of 35 GHz in the high-resolution spectroscopy experiments with CW lasers (see Chapter 6). This inconsistency disappears if one assumes that this high value $\Gamma_{fe} = (1\text{ ps})^{-1}$ only is the relevant value during an intense picosecond optical pulse. We have, however, at this stage no knowledge to support such an assumption. This point therefore needs to be investigated in more detail in future experiments, as well as in work that improves the initial modeling that we present here.

We consider the $D^0 - D^0X$ transitions at $B = 7$ T, this gives the following wavelengths for the optical transitions: $\lambda_A = 8177.0$ Å, $\lambda_{A^*} = 8176.0$ Å, $\lambda_{B^*} = 8176.3$ Å, $\lambda_B = 8175.3$ Å.

For the numerical simulation we assume the absolute values of optical Rabi frequencies to be equal for all transitions if allowed by the polarization selection rules. The Rabi pulse follows the time profile described by a Gaussian function with temporal width $\Delta T = 5$ ps FWHM, and centered around time $t = 0$. The equation of motion for the density matrix of the 4-level system is solved numerically with the electron spin initially in a completely incoherent and depolarized state, which corresponds to $S_x = S_y = S_z = 0$.

Fig. 7.4 shows the transverse spin values S_x and S_y in units of $\hbar$ in the rotating frame as a function of time for optical excitation with three different polarizations: $D+ = \frac{1}{\sqrt{2}}(H+V)$, $\sigma+ = \frac{1}{\sqrt{2}}(H+iV)$ and V. We note that the theoretical maximum for the $S_{x,y}$ component of electron spin was chosen to be $\hbar$.

The $D+$ polarization results in the generation of a large amplitude for the spin S_x component, which was indeed expected from the analysis of the optical dark state in the previous Section. No spin amplitude S_y is generated since it requires a $\pi/2$ phase shift between the Rabi frequencies Ω_1 and Ω_2.

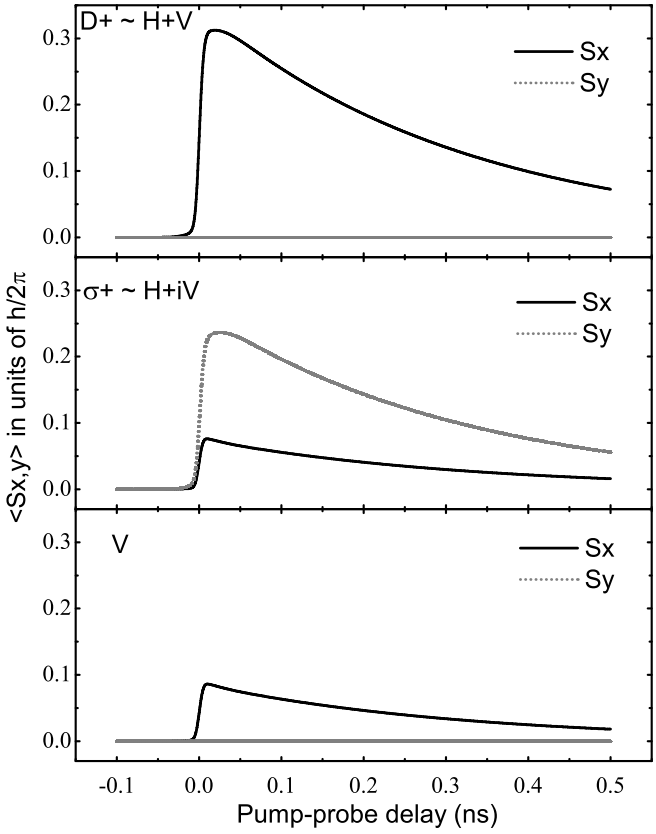

Figure 7.4: Time dependence of the transverse components S_x and S_y of the electron spin in the rotating frame after excitation with the optical pulse, for different polarizations.

In the case of $\sigma+$ polarization, based on the analysis of the optical dark state, the generation of the S_y spin dark state is expected. The simulation results indeed indicate that the S_y component is dominant. The presence of a smaller S_x result from the fact that our 4-level model consists of two Λ-systems, $A-A^*$ and $B-B^*$. Since the polarization selection rules associated with the optical transitions that constitute these two Λ-systems are different, the optical dark state that is gener-

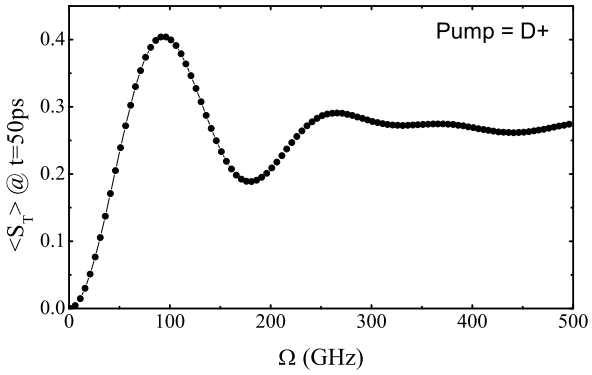

Figure 7.5: Simulation result for the amplitude of the TRKR signal at 50 ps pump-probe delay, as a function of pump pulse power (parameterized by Ω for the value of $\Omega_1 - \Omega_4$).

ated by both systems will also be different. Such, when the A-system favors the S_y spin state upon excitation with $\sigma+$ polarization, the B-system will yield a S_x spin state owing to the fact that both the B and the B^* transition couple to V polarization. The reason that the simulation results show a smaller amplitude for the S_x than the S_y component is due to the fast relaxation within the D^0X complex $\Gamma_{fe} = 1$ ps. The role of this relaxation is to "leak" the optical transition to the $A-A^*$ system which favors the pure S_y state preparation. For even larger $\Gamma_{fe} = (100\text{ fs})^{-1}$ the S_y component will virtually vanish.

Calculations for a purely V-polarized pump result in a small S_x component due to the dark state generation in the $B - B^*$ system. This component also vanishes when the Γ_{fe} relaxation rate is increased by a factor of 10.

The simulation results demonstrate that with strong optical pulses any coherent spin state can be prepared on a time scale that is much shorter than the radiative lifetime. This is a consequence of the coherent dynamics within the 4-level system. When the system is subject to excitation by an intense optical pulse, this induces optical Rabi oscillations in the 4-level system. When the area of the pulse satisfies the condition that $\int \Omega(t)dt = \pi$ (for each transition, *i.e.* $\Omega_1 - \Omega_4$) it will transfer some fraction of the spins from the completely incoherent state, via the states of donor-bound excitons, to the coherent dark state. Since it is relatively easy to induce optical Rabi frequencies that are larger then $1/T_{pulse}$, the ultra-fast population transfer to the spin dark state is possible. The simulated dependence of the transverse spin component on the Rabi frequency induced by a $D+$ polarized pump pulse is shown in Fig. 7.5. In order to achieve a maximum amplitude of the

prepared spin state either the duration or the intensity (which is experimentally is more easy to do) of the optical pulse has to be chosen such that the 4-level system undergoes exactly $(2n+1)/2$ periods of the optical Rabi oscillations.

It is important to note, that in contrast to the traditional optical pumping schemes [12, 15] that prepare spin in a pure spin up or down state, our technique allows for preparation of only a fraction of the electron spins. Inspection of the density matrix from the simulations shows that the ultra-fast preparation of the optically dark state gives a density matrix that is a linear combination of the pure coherent dark state, and a completely incoherent state with substantial population on all levels of the system. The fact that the spin ensembles can not be prepared fully in a dark state, on a timescale that is shorter then the radiative lifetime, is not necessarily a problem, since for many quantum algorithms it is not an amplitude of the coherence, but rather a fidelity with which this coherence can be prepared is important, as is well-established in the field of NMR quantum computing [10, 27].

7.5 Experiment on coherent dark state preparation with single picosecond optical pulses

In order to experimentally investigate the ultra-fast preparation of the coherent dark state in the electron spin ensembles we used the TRKR technique, which is a widely used method to study the dynamics of electron spin ensembles in the conduction band of semiconductors. In a TRKR experiment the system is excited with a polarized optical pulse, which, owing to the polarization selection rules, polarizes the electron spins system [23]. A linearly polarized probe, that comes with delay Δt after the pump arrival, is probing the remaining spin polarization via rotation of its polarization upon reflection. When the experiment is done in a magnetic field and the pump laser polarization is chosen to initially polarize electron spins with a component in the direction orthogonal to the external magnetic field, the spins will undergo a precessing motion and the response of the probe as a function of delay between pump and probe Δt will acquire an oscillatory character. While precessing, the initially polarized electron spin ensemble will be subject to energy relaxation that is characterized by the spin relaxation time T_1 and spin dephasing that is characterized by the spin dephasing time T_2^*. The "*" indicates here that it is a dephasing of the spin ensemble rather than the decoherence of an individual electron spin which loses its coherence over a time T_2.

The TRKR technique is widely used for exploring the dynamics of electron spins in the conduction band of bulk GaAs and two dimensional electron gas (2DEG) systems in GaAs/AlGaAs heterostructures [19, 21, 22]. In those experiments a cir-

cularly polarized light with a photon energy above the gap is used to polarize the electron spins in the conduction band [23]. Owing to the polarization selection rules fr bulk GaAs and 2DEG electrons, spins are being polarized along the light propagation direction, which is therefore often chosen to be orthogonal to the applied magnetic field (the so-called Voigt geometry).

It is important to note that the spin polarization due to above-gap optical excitation is a single photon process with optical generation of a free electron-hole pair. This, in turn, sets a challenge on applying a TRKR technique for studying the dynamics of the electron spins of D^0 systems, since the single photon process gives in this case excitation of the donor-bound exciton complex D^0X. Notably, this state carries no electron-spin angular momentum since the electrons form a singlet.

In order to polarize the donor-bound electron spin one has to rely on a two-photon stimulated Raman process which is the exact process that was described previously in this Chapter. Under strong excitation from a polarized optical pulse the ensemble of D^0 electron spins is polarized according to the ultra-fast dynamics of the coherent dark state preparation.

We performed our experiment using conventional [19, 22] mono-color time-resolved Kerr-rotation measurements in an optical cryostat at 4.2 K with magnetic fields (magnitude B) up to 7 T. We used a tunable Ti:sapphire laser with ~150 fs pulses at 80 MHz repetition rate. The spectrum of pulses was narrowed with a help of tunable liquid crystal Fabry-Perot filters, resulting in pulses with a spectral width $\Delta\lambda$ = 1 nm and duration of approximately T_{pulse} = 5 ps. The central wavelength of the pulses was chosen to be close to resonance with the $D0-D^0X$ transitions, which is λ_c = 817.5 nm at B = 7 T. Samples were excited at normal incidence. In initial measurements we employed a lock-in detection scheme with intensity modulation for the train of pump pulses (with an optical chopper at a few kHz), at constant pump polarization. For later measurements we used a lock-in scheme with polarization modulation for the pump, with a photoelastic modulator at 50 kHz. This yields better signal-to-noise, and we first confirmed that we could still unambiguously derive the dependence on pump polarization. We were able to modulate the polarization either between $\sigma+/\sigma-$, $D+/D-$, or H/V, in order to cover all important polarization states on the Poincare polarization sphere. This creates spin orientation for the donor-bound electrons ensemble due to the coherent-dark-state formation. The evolution of the spin ensemble is recorded by measuring the Kerr rotation of a reflected probe pulse with a polarization bridge, at the frequency of the pump modulation. Measuring this as a function of pump-probe delay Δt yields the TRKR traces. The polarization of the probe could also be chosen arbitrarily. We used spot diameters of about 100 μm, and data was taken at different pump-photon densities in order to cover a broad range of values for the

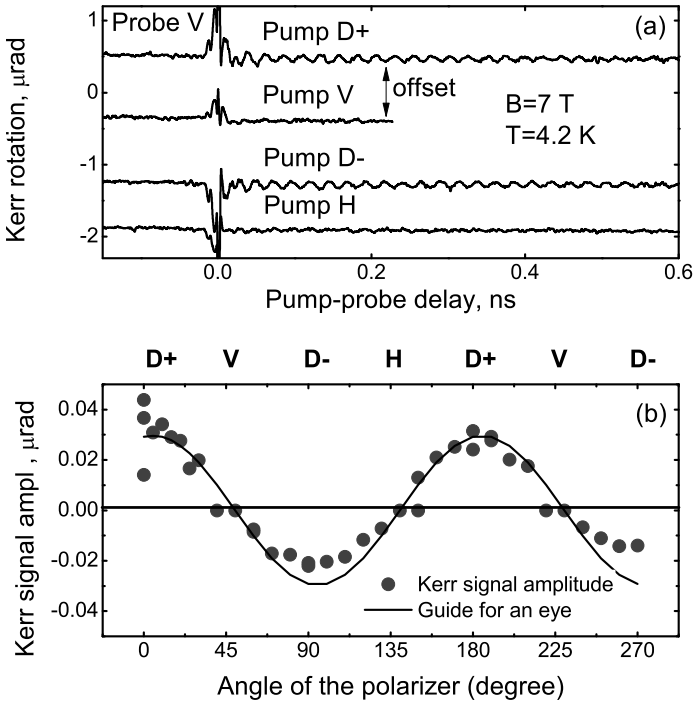

Figure 7.6: (a) TRKR signal for different polarizations of the pump pulse. The probe is V polarized. Traces are offset for clarity. (b) Amplitude of the TRKR signal as a function of the orientation of the linear polarization of the pump with respect to the applied magnetic field, expressed in degree units for the angle of the polarizer.

optical Rabi frequencies. Unless states otherwise, we present data that is taken in a field of $B = 7$ T and at a temperature of 4.2 K.

Experimental results taken on a sample with Si donors at a concentration of $n_{Si} = 3 \times 10^{13}$ cm^{-3} are shown in Fig. 7.6. Panel (a) shows the TRKR response of a V polarized probe for different linear polarizations for the pump. When the pump is $D+/D-$ polarized, it results in a non-zero oscillating Kerr amplitude, while for the H/V polarized pump no Kerr oscillations are observed. Panel (b) of Fig. 7.6 shows the full dependence of the amplitude of Kerr oscillations (evaluated around $\Delta t =$ 50 ps) as a function of the orientation of the linear polarization of the pump with respect tot the magnetic field. The observed results are in a good agreement with

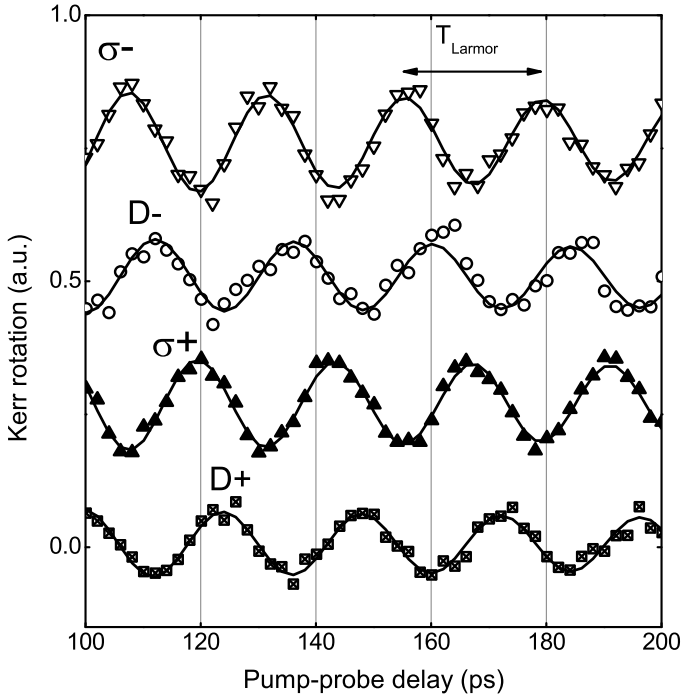

Figure 7.7: TRKR response of the D^0 spin ensemble, for different polarizations of the pump pulse. The $\pi/2$ phase difference between TRKR oscillations from pumping with $D+$ and $\sigma+$ polarization indicates the initial preparation of spin S_x and the spin S_y states, respectively. The probe was V polarized.

our theoretical description of the formation of a coherent dark state via a 2-photon stimulated Raman process, and its dependence on the polarization selection rules. For creating spin coherence in the D^0 system, the system demands both an H- and V-polarized component in the pump pulse, in order to address both electron spin states simultaneously. The fact that no spin coherence was created when pumping with V polarized light confirms our assumption that the $B-B^*$ Λ-system, which in general can lead to stimulated Raman processes with a V-polarized component of the pump only, is shunted by the fast relaxation rate Γ_{fe}.

Next we proceed with demonstrating that by controlling polarization state of the pump we can create any arbitrary spin state for the D^0 system. In the presentation we limit ourself to the generation of 4 spin states in the equatorial plane of

the Bloch sphere, which are the states of the the maximum coherence. These are the $\pm S_x$ and the $\pm S_y$ spin states, and these are the dark states for pumping with the $D+/D-$ and $\sigma+/\sigma-$ polarizations, respectively. The TRKR traces from these measurement are shown in Fig. 7.7. The phase of the oscillating TRKR traces taken at a fixed pump-probe delay ($\Delta t = 100$ ps, for example) directly reflects the initial phase of the TRKR response, and therefore the actual orientation of the coherent dark state that was prepared by the pump pulse.

The results of the experiment of Fig. 7.7 are in a good agreement with our theory for the ultrafast preparation of coherent dark states. The four optical polarizations in use, when presented on the Poincare sphere, have a phase difference $\pi/2$ between neighboring polarization vectors. The TRKR oscillation signals that correspond to these four cases demonstrate the same phase shift of $\pi/2$ for the sequence $\sigma-$, $D-$, $\sigma+$ and $D+$. This directly follow from the polarization selection rules. The $D+ = \frac{1}{\sqrt{2}}(H+V)$ polarization results in the $|S_x\rangle = \frac{1}{\sqrt{2}}(|\uparrow\rangle + |\downarrow\rangle)$ coherent dark state, the $\sigma+ = \frac{1}{\sqrt{2}}(H+iV)$ polarization on the other hand will yield the $|S_y\rangle = \frac{1}{\sqrt{2}}(|\uparrow\rangle + i|\downarrow\rangle)$ state, etc. When presented on the Bloch sphere, the phase difference between the spin states S_x and S_y is also $\pi/2$. With this experiment we therefore have demonstrated a direct mapping of the polarization state vector of the Poincare sphere onto the spin state vector of the Bloch sphere.

We also checked that the amplitude of TRKR traces is consistent with varying the relative intensity of the H and V components in the pulse, which varies the ratio $|\Omega_1|/|\Omega_2|$ for the dark state (data not shown). This gives access to preparing spin states that are tilted upward or downward from the equatorial plane of the Bloch sphere, and confirms our technique can prepare any spin state.

This technique is an interesting alternative to preparing spin states via conventional optical pumping. Firstly, it allows for direct preparation of an arbitrary state. Optical pumping can only prepare the pure spin-up or spin-down state, and needs a subsequent step with coherent spin manipulation for preparing an arbitrary state. In addition, our technique is about 1000 times faster. Conventional optical pumping requires a time that corresponds to a few cycles of the radiative lifetime $T_{rad} = 1$ ns, while our stimulated Raman technique can be realized with an optical pulse of $T_{pulse} \lessapprox 5$ ps, provided that the optical Rabi frequency during the pulse is high (giving at least a pulse area of the order π).

We can estimate the optical Rabi frequencies using the electrical dipole value that we estimated from the EIT observation in Chapter 6 ($\Omega/2\pi = 2$ GHz for $P = 10$ W/cm^2). In this pulsed experiment the maximum available pump power was $P = 10$ mW, with a spot size $D_{spot} \approx 100$ μm, and 80 MHz repetition rate of pulses with $T_{pulse} \approx 5$ ps duration. This corresponds to an optical intensity of about $I \approx 3 \cdot 10^5$ W/cm^2, resulting in the integrated Rabi frequency $\Omega/2\pi = 350$ GHz, and

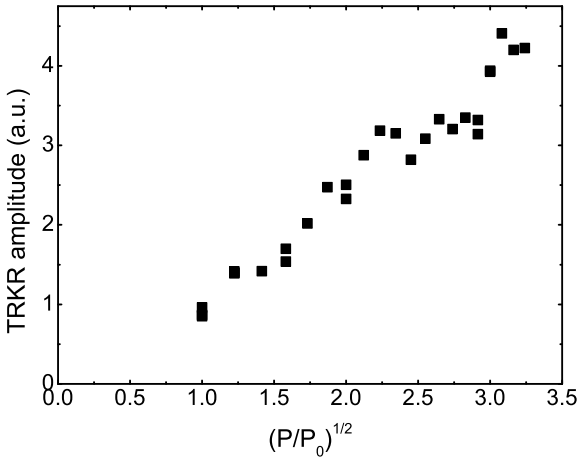

Figure 7.8: Experimentally measured amplitude of the TRKR oscillations as a function of the pump pulse power (P_0 = 1 mW). Measurements were done with a $\sigma+$ polarized pump and a V-polarized probe.

a pulse area of about π. It is, however, important to note that this estimate is quite rough, since the estimates for the spot size and the optical power loss on the windows of the cryostat have not been processed with good accuracy yet.

As was mentioned earlier, the ultra-fast preparation of the coherent dark state is possible because of the optical Rabi oscillations that take place in the system when a strong optical pulse is present. This should, according to the results of the calculation in Fig. 7.5, lead to a Kerr signal amplitude that is a strong function of the excitation pulse power. Figure 7.8 shows the amplitude of the TRKR signal measured as a function of the pump intensity for $\sigma+$ pump polarization. It demonstrates a steady monotonous increase in the Kerr signal amplitude. The fact that no oscillating-like behavior is observed does not allow us to estimate how close we are to the full π Rabi pulse. Attempts to see more then π Rabi pulses were limited by the available laser power.

7.6 Probing the coherent optical dark state

So far we have shown that by choosing the right polarization for the optical pump pulse, any coherent dark state for the D^0 spin ensemble can be prepared. This

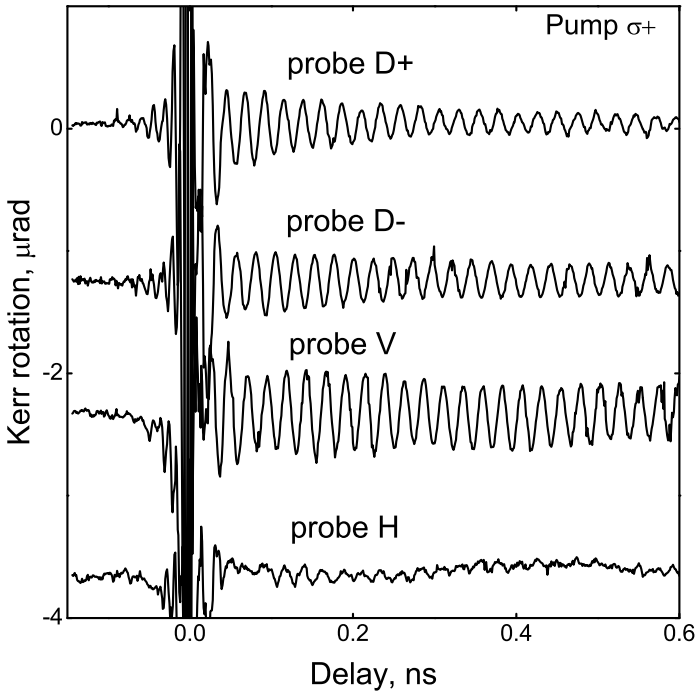

Figure 7.9: Dependence of the TRKR signal on the polarization of the probe. The pump pulse is chosen to be $\sigma+$ polarized.

happens only when the optical pulse can drive a Raman-like two-photon transition between the two electron spin levels. In the TRKR experiment that we presented till here, we have probed the dynamics of this dark state by measuring how the rotation of an initially V-polarized probe rotates upon reflection. For complete understanding of the interaction between D^0 systems and ultra-fast optical pulses it is of interest to also investigate the dependence on the initial polarization of the probe pulse.

For studying this, we have performed TRKR experiments where the pump pulse was chosen to be $\sigma+$ polarized, while polarization of the probe was chosen to be $D+$, $D-$, V or H. Results of this experiment are shown in Fig. 7.9. The most interesting observation is the fact that, in contrast to the other three polarizations, the H polarized probe leads to a Kerr signal that is much weaker than for the other

probe polarizations. Considering that the H polarization is the only polarization that couples only to one optical transition in the 4-four level system of Fig. 7.2, we conclude that the process of probing the spin dynamics is also a two-photon process.

A two-photon interaction between the probe pulse and the D^0 systems is indeed necessary if one wants to observe an oscillating Kerr signal that contains information about the spin state that precesses in external magnetic field. If one has a probe polarization that is sensitive to only one of the optical transitions, it would lead to probing either the population of the $|\uparrow\rangle$ or $|\downarrow\rangle$ state. This concerns eigenstates of the $\hat{S}_z$ operator, and these do not precess. It is the terms of the density matrix of the type $|\uparrow\rangle\langle\downarrow|$ that are time dependent, and probing this time dependence requires simultaneous probing of $|\uparrow\rangle$ and $|\downarrow\rangle$ states in order to capture the time dependence in a physically observable parameter, as for example the Kerr rotation of the probe polarization.

The other interesting observation from the experimental results in Fig. 7.9 is a relatively high Kerr amplitude for the V-polarized probe. The V probe polarization can indeed provide a necessary two-photon process via the optical transitions in the $B-B^*$ Λ-system in Fig. 7.1. In contrast to pumping, where the pure V polarization gives no D^0 spin coherence due to the shunting of the $B-B^*$ by the fast relaxation Γ_{fe}, probing with V polarization gives a clear Kerr signal. The reason is that rotation of the probe polarization can still occur, because the actual absorption and effective index of refraction is sensitive to the one-photon absorbtion processes for each leg of the Λ system, and these are still sensitive to a quantum interference between the two transitions.

7.7 Time resolved study of the coherence of electron spin bound to the neutral donor

We conclude this Chapter by presenting an experimental study which aimed at investigating how the spin dephasing time of D^0 spin ensembles depends on the power of the optical excitation. This experimental work was mainly driven by two factors. First, in the experiments with detuned optical pulses [12] that aimed at achieving deterministic spin rotation, the rotation angle was limited to $\pi/3$. It was assumed that larger rotation angles were not possible due to optical-pulse induced dephasing for the optical transitions at high powers. A second reason to perform the experiment is the fact that, up to our knowledge, there was no dedicated TRKR study yet of the dynamics of donor-bound electron spins. The lack of experimental work on the dynamics of the donor bound electrons is not due to the limited

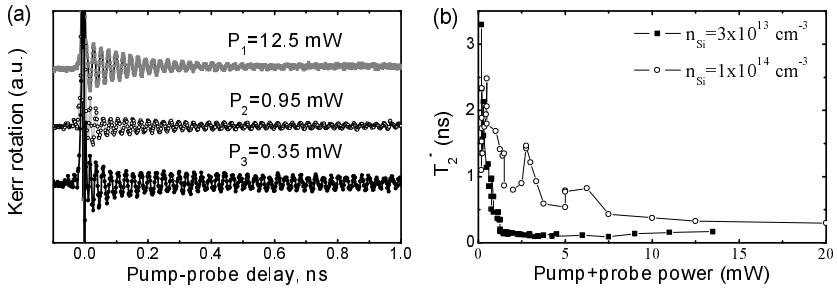

Figure 7.10: (a) TRKR signals for different pump powers P, taken on a sample with Si doping at $n_{Si} = 3 \times 10^{-13}$ cm^{-3}, and $\sigma+$ and V for the pump and probe polarization, respectively. (b) Spin dephasing time T_2^* versus pump power for samples with different concentration of donors.

interest in this system, but rather due to the fact, that the conventional Kerr rotation technique (with above the gap excitation) was mainly used for studies of electrons in the conduction band of semiconductors, where generation of electron spin coherence is a one-photon process [19]. Another technique, that uses polarization-resolved photo-luminescence in combination with the Hanle effect [28] cannot address the donor-bound electrons since the part of the signal that comes from the radiative relaxation of D^0X systems is not polarized because the electron spins in the D^0X system form a singlet.

We have performed the TRKR experiment on two samples with different concentration of dopants $n_{Si} = 3 \times 10^{13}$ cm^{-3} and $n_{Si} = 1 \times 10^{14}$ cm^{-3}. Experiments were performed using different excitations powers. Results are presented in Fig. 7.10. Panel (a) shows typical TRKR traces taken at three different pump power levels. It is interesting to note that the spin signal after excitation with the lowest pump level persists longer than for the cases with stronger pumping. In panel (b) we present the result of a systematic study of the dependence of the spin sephasing time T_2^* on the excitation power for the two samples. The T_2^* time for each power condition was found from making a mono-exponential fit on the Kerr signal [21, 22]. The behavior of the spin dephasing times T_2^* versus pump power shows a trend where T_2^* initially decreases exponentially with increasing of the optical power. At the high power levels the dephasing time stays nearly flat at the value $T_2^* \approx 0.2$ ns. The point where the change in the trend occurs is at the power level where the number of absorbed pump photons equals the number of D^0 donor sites.

The observed results are in good agreement with a model that predicts that the spin coherence time is limited by the correlation time of the local effective magnetic field felt by the electron spin. The D^0 system has an unpaired electron spin, and it will sense the non-zero hyperfine interaction at the donor site and therefore an Overhauser magnetic field. Slowly changing fluctuations of this Overhauser field cause an inhomogeneity for the Zeeman splitting of the D^0 systems, and this should result in a value $T_2^* \approx 2$ ns. This is the T_2^* value that is observed at the lowest pump powers. At higher pump powers, there are also a relatively high number of free excitons X in the system, up to a time that corresponds to the free-exciton recombination time (~300 ps [21]). These free excitons have at 4.2 K a capture and release dynamics with being bound at a D^0 site, temporarily forming a D^0X system. For the D^0X system, the two electrons form a singlet, resulting in no Overhauser field. Thus the capture and release of the free excitons creates an additional fluctuating magnetic field that is felt by the electron, and it can also cause a full electron spin-flip for the D^0 system in case the electron is exchanged.

The dynamics of the capture and release of the free excitons depends on the number of free excitons in the system. In the low pump-power regime the number of free excitations in the system does not strongly exceed the number of donors. This gives a low rate for capture-release events, and a high number of D^0 systems for which the spin dynamics is not disturbed by free excitons. In the case of higher optical pump powers, the number of optical excitations exceeds the number of donors and many free excitons are generated alongside the spin orientation of D^0 systems. Subsequent capture-release dynamics disturbs the D^0 spin dynamics. The effect of this on the spin dephasing time is captured by the following correlation [28]:

$$T_2^* \sim \langle \vec{S}_i(0)\, \vec{S}_i(t) \rangle \sim e^{-t/T_{cap}} \tag{7.5}$$

which, considering the free exciton capture rate must be in the sub-ns range which is supported by the strong luminescence from the donor bound excitons, results in a T_2^* value that is much shorter than the nuclear-field-limited value of $T_2^* \approx 2$ ns.

7.8 Conclusions

We have presented an experimental technique that allows optical generation of an arbitrary coherent state for D^0 spin ensembles on a timescale that is much shorter than the radiative lifetime. We have developed a theoretical model which relies on describing the $D^0 - D^0X$ system as a 4-level system, and which thereby consists of two optical Λ-systems. Within the framework of this model we were able to show that the mechanism of the ultra-fast coherent dark state preparation relies

on a two-photon stimulated Raman process. Despite being able to explain most of the results, we had to introduce an ultra-fast timescale for the relaxation between levels within the D^0X complex, in order to account for a difference in the system's response with respect to preparing and probing states with ultrafast optical pulses with well-defined polarizations. The reported theoretical model and experiments also do not address the question how the coherent dark states evolves when a second pump pulse is applied shortly after a first pump pulse (faster than T_2^*). such that pumping occurs on a system with an initial degree of coherence. More experimental and theoretical investigations in this direction will provide important test for better understanding of the physics that is reported in this Chapter.

Using the developed technique we were also able to make a systematic time-resolved study of the spin dynamics of an ensemble of oriented D^0 spins. Our findings demonstrate that by resonantly exciting the $D^0 - D^0X$ transitions with single optical pulses, a detectable and well-defined electron spin coherence can be generated, and its dynamics can be traced in time. We have also found that the spin coherence time is strongly dependent on the number of photons in the pump pulse, and in general decreases with increasing power.

References

[1] T. D. Ladd, F. Jelezko, R. Laflamme, Y. Nakamura, C. Monroe, and J. L. O'Brien, *Quantum computers.*, Nature **464**, 45 (2010), ISSN 1476-4687.

[2] E. Knill, R. Laflamme, and G. J. Milburn, *A scheme for efficient quantum computation with linear optics.*, Nature **409**, 46 (2001), ISSN 0028-0836.

[3] R. Blatt and D. Wineland, *Entangled states of trapped atomic ions.*, Nature **453**, 1008 (2008), ISSN 1476-4687.

[4] R. Hanson, J. R. Petta, S. Tarucha, and L. M. K. Vandersypen, *Spins in few-electron quantum dots*, Reviews of Modern Physics **79**, 1217 (2007), ISSN 0034-6861.

[5] D. Press, T. D. Ladd, B. Zhang, and Y. Yamamoto, *Complete quantum control of a single quantum dot spin using ultrafast optical pulses.*, Nature **456**, 218 (2008), ISSN 1476-4687.

[6] B. E. Kane, *Silicon-Based Nuclear Spin Quantum Computer*, Nature **393**, 133 (1997).

[7] M. V. G. Dutt, L. Childress, L. Jiang, E. Togan, J. Maze, F. Jelezko, A. S. Zibrov, P. R. Hemmer, and M. D. Lukin, *Quantum register based on individual electronic and nuclear spin qubits in diamond.*, Science (New York, N.Y.) **316**, 1312 (2007), ISSN 1095-9203.

[8] L. M. Vandersypen, M. Steffen, G. Breyta, C. S. Yannoni, M. H. Sherwood, and I. L. Chuang, *Experimental realization of Shor's quantum factoring algorithm using nuclear magnetic resonance.*, Nature **414**, 883 (2001), ISSN 0028-0836.

[9] S. Braunstein, C. Caves, R. Jozsa, N. Linden, S. Popescu, and R. Schack, *Separability of Very Noisy Mixed States and Implications for NMR Quantum Computing*, Physical Review Letters **83**, 1054 (1999), ISSN 0031-9007.

[10] D. G. Cory, A. F. Fahmy, and T. F. Havel, *Ensemble quantum computing by NMR spectroscopy.*, Proceedings of the National Academy of Sciences of the United States of America **94**, 1634 (1997), ISSN 0027-8424.

[11] J. H. Plantenberg, P. C. de Groot, C. J. P. M. Harmans, and J. E. Mooij, *Demonstration of controlled-NOT quantum gates on a pair of superconducting quantum bits.*, Nature **447**, 836 (2007), ISSN 1476-4687.

[12] K.-M. C. Fu, S. M. Clark, C. Santori, C. R. Stanley, M. C. Holland, and Y. Yamamoto, *Ultrafast control of donor-bound electron spins with single detuned optical pulses*, Nature Physics **4**, 780 (2008), ISSN 1745-2473.

[13] S. Clark, K.-M. Fu, T. Ladd, and Y. Yamamoto, *Quantum Computers Based on Electron Spins Controlled by Ultrafast Off-Resonant Single Optical Pulses*, Physical Review Letters **99**, 040501 (2007), ISSN 0031-9007.

[14] S. Clark, K.-M. Fu, Q. Zhang, T. Ladd, C. Stanley, and Y. Yamamoto, *Ultrafast Optical Spin Echo for Electron Spins in Semiconductors*, Physical Review Letters **102**, 247601 (2009), ISSN 0031-9007.

[15] X. Xu, Y. Wu, B. Sun, Q. Huang, J. Cheng, D. G. Steel, A. S. Bracker, D. Gammon, C. Emary, and L. J. Sham, *Fast Spin State Initialization in a Singly Charged InAs-GaAs Quantum Dot by Optical Cooling*, Physical Review Letters **99**, 97401 (2007), ISSN 0031-9007.

[16] M. Atatüre, J. Dreiser, A. Badolato, and A. Imamoglu, *Observation of Faraday rotation from a single confined spin*, Nature Physics **3**, 101 (2007), ISSN 1745-2473.

[17] J. Berezovsky, M. H. Mikkelsen, N. G. Stoltz, L. A. Coldren, and D. D. Awschalom, *Picosecond coherent optical manipulation of a single electron spin in a quantum dot.*, Science (New York, N.Y.) **320**, 349 (2008), ISSN 1095-9203.

[18] K.-M. Fu, C. Santori, C. Stanley, M. Holland, and Y. Yamamoto, *Coherent Population Trapping of Electron Spins in a High-Purity n-Type GaAs Semiconductor*, Physical Review Letters **95**, 187405 (2005), ISSN 0031-9007.

[19] J. Kikkawa and D. Awschalom, *Resonant Spin Amplification in n-Type GaAs*, Physical Review Letters **80**, 4313 (1998), ISSN 0031-9007.

[20] P. J. Rizo, A. Pugzlys, J. Liu, D. Reuter, A. D. Wieck, C. H. van der Wal, and P. H. M. van Loosdrecht, *Compact cryogenic Kerr microscope for time-resolved studies of electron spin transport in microstructures.*, The Review of scientific instruments **79**, 123904 (2008), ISSN 1089-7623.

[21] P. J. Rizo, A. Pugzlys, A. Slachter, S. Z. Denega, D. Reuter, A. D. Wieck, P. H. M. van Loosdrecht, and C. H. van der Wal, *Optical probing of spin dynamics of two-dimensional and bulk electrons in a GaAs/AlGaAs heterojunction system*, Accepted for publication in New J. Phys, arXiv:0910.1714 (2009).

[22] S. Z. Denega, T. Last, J. Liu, A. Slachter, P. J. Rizo, P. H. M. van Loosdrecht, B. J. van Wees, D. Reuter, A. D. Wieck, and C. H. van der Wal, *Suppressed spin dephasing for two-dimensional and bulk electrons in GaAs wires due to engineered cancellation of spin-orbit interaction terms*, Physical Review B **81**, 153302 (2010), ISSN 1098-0121.

[23] F. Meier and B. P. Zakharchenya, *Optical Orientation* (North Holland Physics Publishing, 1984).

[24] V. A. Karasyuk, D. G. S. Beckett, M. K. Nissen, A. Villemaire, T. W. Steiner, and M. L. W. Thewalt, *Fourier-transform magnetophotoluminescence spectroscopy of donor-bound excitons in GaAs*, Physical Review B **49**, 16381 (1994), ISSN 0163-1829.

[25] M. Sladkov, A. U. Chaubal, M. P. Bakker, A. R. Onur, D. Reuter, A. D. Wieck, and C. H. van der Wal, *Electromagnetically Induced Transparency with an Ensemble of Donor-Bound Electron Spins in a Semiconductor*, Phys. Rev. B **82**, 121308(R) (2010).

[26] K.-M. Fu, W. Yeo, S. Clark, C. Santori, C. Stanley, M. Holland, and Y. Yamamoto, *Millisecond spin-flip times of donor-bound electrons in GaAs*, Physical Review B **74**, 121304 (2006), ISSN 1098-0121.

[27] N. A. Gershenfeld and I. L. Chuang, *Bulk Spin-Resonance Quantum Computation*, Science **275**, 350 (1997), ISSN 00368075.

[28] R. Dzhioev, K. Kavokin, V. Korenev, M. Lazarev, B. Meltser, M. Stepanova, B. Zakharchenya, D. Gammon, and D. Katzer, *Low-temperature spin relaxation in n-type GaAs*, Physical Review B **66**, 245204 (2002), ISSN 0163-1829.